

## RESEARCH PAPER

## Production of chrome-manganese ligature using ferrosilicochrome dust as a reducing agent

Sultan Kabylkanov<sup>\*1,2</sup>, Yerbolat Makhambetov<sup>1</sup>, Saule Abdulina<sup>2</sup>, Azamat Burumbayev<sup>1</sup>, Armat Zhakan<sup>1</sup>, Yucel Onuralp<sup>3</sup>

<sup>1</sup> Chemical-Metallurgical Institute named after Zh. Abishev, Yermekov street 63, 100009, Karaganda, Kazakhstan

<sup>2</sup> East Kazakhstan Technical University named after D. Serikbayev, Serikbayev street 19, 070000, Ust-Kamenogorsk, Kazakhstan

<sup>3</sup> Istanbul Technical University, Buyukdere street 2, 34467, Istanbul, Turkey

\*Corresponding authors: [kabyl\\_96@mail.ru](mailto:kabyl_96@mail.ru) / Chemical-Metallurgical Institute named after Zh. Abishev, Yermekov street 63, 100009, Karaganda, Kazakhstan / D. Serikbayev East Kazakhstan Technical University, Serikbayev street 19, 070000, Karaganda, Kazakhstan

Received: 26.06.2025

Accepted: 21.07.2025

## ABSTRACT

This article presents the results of thermodynamic modeling of the process of obtaining chromium-manganese ligature from ferro-manganese ore and dust from crushing ferrosilicochrome (FeSiCr). The calculations were performed using the "HSC Chemistry" software package, where dust from crushing FeSiCr was used as a reducing agent. The analysis was performed by varying the reducing agent dust FeSiCr from 10 to 100 kg in increments of 10 kg per 100 kg of ferro-manganese ore, at temperatures of 1400 °C, 1600 °C and 1800 °C. The mechanism of combined metallothermic reduction of chromium (Cr), manganese (Mn), and iron (Fe) was studied in a multicomponent Fe-Cr-Mn-Si-Al-Ca-Mg-O system. Based on thermodynamic data, it was found that the optimal consumption of reducing agent is 50 kg per 100 kg of ore, and the most effective melting temperature is 1600 °C, at which the best yield of chromium-manganese ligature is achieved. Additionally, laboratory tests were conducted under specific conditions, resulting in experimental samples of the ligature with the following chemical composition, %: Fe – 28.39, Cr – 16.58, Mn – 32.55, Si – 3.56.

**Keywords:** chrome-manganese ligature, temperature, thermodynamic modelling, ferrosilicochrome dust, metallothermic reduction.

## INTRODUCTION

In recent decades, global steel production has experienced steady growth, driven not only by advancements in mechanical engineering, construction, and the defence industry, but also by global technological trends that have led to increasing demands for high-quality metal products. This, in turn, has led to a significant rise in the demand for various ferroalloys and alloying additives, which are essential components in the production of high-grade steels. Among these, chrome-manganese ligatures have gained particular importance due to their ability to enhance the mechanical properties, wear resistance, corrosion resistance, and thermal stability of steels [1].

In the field of ferrous metallurgy, chromium- and manganese-containing alloys are regarded as strategically important and irreplaceable alloying components with virtually unlimited application potential. They are widely used in steels of various grades – from structural to highly alloyed tool steels, including heat-resistant and stainless steels. These alloys are particularly in demand for the production of high-strength structural materials utilised in heavy machinery, aerospace engineering, railway infrastructure, and the energy sector.

In the context of the Republic of Kazakhstan, which possesses substantial but largely underutilised reserves of chromium and manganese ores, the development of efficient processing technologies and alloy production methods is particularly relevant [2-4]. Specifically, the exploitation of local ores with high impurity content and low metallurgical grade can be realised through the implementation of innovative approaches to the smelting of chrome-manganese ligatures.

The objective of this study is to conduct a scientifically grounded investigation and develop the technological foundations for aluminosilicothermic smelting of a chrome-manganese alloy using a novel, domestically produced silicon-aluminium ferroalloy as the reducing agent. The primary goal is to involve low-grade chromium- and manganese-containing ores, previously unused in ferroalloy production, in metallurgical processing to obtain an alloy with a specified chemical composition and a high recovery rate of target elements [5].

To achieve this objective, the primary oxidised component used is a low-grade ferro-manganese ore from the Kerege-Tas deposit, located in central Kazakhstan. As a reducing agent, ferrosilicochrome (FeSiCr) dust is employed – this material is generated during the crushing and processing of ferroalloys. It is characterised by its fine dispersion and high content of active elements such as silicon, chromium, and iron. The use of this secondary material significantly reduces

production costs and supports the broader goal of efficiently utilising industrial waste.

Thermodynamic modelling, as a modern tool for predicting the behaviour of multicomponent systems, is based on fundamental laws of physics and chemistry and is used for the quantitative analysis of energy and phase transformations occurring during chemical reactions [6–9]. This method is particularly effective in the study of complex reduction processes in metallurgy, including the development of new alloying systems and ligatures [10–12]. To determine the optimal parameters for smelting chrome-manganese ligature, a comprehensive thermodynamic analysis of the system was conducted. This allowed the identification of the most probable directions of reduction reactions, their energetic efficiency, and the expected phase composition of the products. The analysis took into account the specifics of the multicomponent initial charge, which included ferro-manganese ore, FeSiCr dust as the reducing agent, and lime as the fluxing additive.

Particular attention in this study was devoted to an in-depth analysis of the mechanism of combined metallothermic reduction of chromium and manganese oxides within the complex multicomponent Fe-Cr-Mn-Si-Al-Ca-Mg-O system. This approach is essential for understanding the sequence and competitiveness of reduction reactions that occur between various oxide species and the active reducing components – primarily silicon and aluminium from the silicon-aluminium ferroalloy. The consideration of phase transformations and potential side reactions involving calcium, magnesium, and other elements in the system allowed for the identification of the most probable pathways for metallic phase formation, as well as the formation of slag compounds [13].

To validate the results of thermodynamic modelling and to obtain experimental data reflecting the actual behaviour of the system under high-temperature conditions, laboratory-scale smelting experiments were conducted using a Tammann-type electric furnace. During these experiments, process parameters such as temperature regime, charge composition, and the mass ratios between the reducing agents and oxidised components were systematically varied. The outcomes of the experiments not only confirmed the theoretical predictions but also enabled the refinement of optimal technological conditions, ensuring the maximum recovery of chromium and manganese into the metallic phase and the formation of a favourable slag composition with minimal losses.

The developed chrome-manganese ligature, obtained from local ores and secondary materials, demonstrates not only a high recovery rate of target elements but also strong potential for further processing and refining. The study's results

confirm the high resource efficiency of the proposed technology, its economic viability, and export potential, making it a relevant direction for advancing Kazakhstan's ferroalloy industry.

Thus, the implementation of the developed technology can contribute not only to the rational utilisation of Kazakhstan's mineral resource base but also to the creation of value-added products through the processing of low-grade and secondary raw materials. Moreover, it supports the improvement of environmental performance in metallurgical processes by reducing waste generation and increasing the efficiency of resource utilisation. This, in turn, facilitates the expansion of the range of competitive metallurgical products targeted at both domestic and international markets, strengthening Kazakhstan's position in the global ferroalloy industry.

## MATERIAL AND METHODS

Thermodynamic modelling was carried out using ferro-manganese ore from the "Keregetas" deposit as the main raw material and FeSiCr dust as the reducing agent. The chemical composition of these materials is presented in **Tables 1 and 2**.

**Table 1** Chemical composition of ferro-manganese ore, %

Mn <sub>common</sub>	Fe <sub>2</sub> O <sub>3</sub>	SiO <sub>2</sub>	Al <sub>2</sub> O <sub>3</sub>	MgO	CaO	P <sub>2</sub> O <sub>5</sub>	S
26.62	21.78	16.74	2.57	0.15	2.34	0.43	0.17

**Table 2** Chemical composition of FeSiCr dust, %

Cr	Fe	Si	Al	C	S	P
24.10	14.18	32.22	1.51	2.48	0.049	0.018

To calculate the coexisting phases in the Fe-Cr-Mn-Si-Al-Ca-Mg-O system, thermodynamic data from the "HSC Chemistry 6" database were used. This database is part of the comprehensive "HSC Chemistry 6" software package, which is regularly updated in accordance with the Scientific Group for Thermodynamic Data (SGT) standards. According to sources [14–17], the error margin when using the HSC Chemistry software does not exceed 4–6%. This level of accuracy is considered acceptable for most metallurgical and other scientific and engineering applications.

HSC Chemistry is a powerful software tool that enables thermodynamic calculations to be performed on personal computers with high speed and accuracy [18–20]. The HSC software is widely used in scientific research, educational institutions, and industry for optimising various processes such as metallurgy, chemical production, and the development of new materials [21, 22].

To calculate phase equilibria in multicomponent systems such as Fe-Cr-Mn-Si-Al-Ca-Mg-O, the "Equilibrium Compositions" module was used. This module enables the modelling of phase compositions that are in equilibrium under specified conditions of temperature, pressure, and system composition. This is essential for accurately determining the composition and properties of various phases.

To calculate the minimum Gibbs free energy, which characterises the equilibrium state of the system, the "GIBBS" program algorithm was used. This method enables the determination of optimal conditions for chemical reactions and phase formation by minimising the total energy of the system. The Gibbs algorithm is a key method for modelling chemical reactions and phase transitions in metallurgy and other fields that require precise thermodynamic calculations.

For conducting thermodynamic analysis, the following fundamental principles are formulated, which form the basis for modelling the Fe-Cr-Mn-Si-Al-Ca-Mg-O system using FeSiCr dust as the reducing agent:

1. Temperature regime. The calculations consider temperatures of 1400°C, 1600°C, and 1800°C to conduct a comparative analysis and determine the optimal conditions for reduction and phase formation.
2. Pressure. In all modelled scenarios, the pressure is assumed to be 0.1 MPa, corresponding to one physical atmosphere [23–25].
3. Volume. The system volume is determined based on its thermodynamic state and composition, assuming a uniform distribution of components among the phases.
4. System type. The system is treated as closed, without mass transfer or heat exchange with the external environment. This allows focusing on the internal thermodynamic interactions of the components.
5. Amount of reducing agent. The effect of the amount of introduced FeSiCr dust is modelled in the range of 10 to 100 kg in 10 kg increments. This variation enables the evaluation of the degree of Cr and Mn reduction, as well as the phase composition of the products, depending on the amount of reducing agent. The

composition of the initial charge mixture used for thermodynamic modelling in the "HSC Chemistry 6" software is presented in **Table 3**.

**Table 3** Composition of the initial charge mixture, kg

Mn <sub>2</sub> O <sub>3</sub>	Fe <sub>2</sub> O <sub>3</sub>	SiO <sub>2</sub>	Al <sub>2</sub> O <sub>3</sub>	MgO	CaO	Fe	Si	Cr
46.77	26.60	20.45	3.14	0.18	2.86	2.01	4.57	3.42
						4.02	9.14	6.84
						6.03	13.71	10.26
						8.05	18.28	13.67
						10.06	22.85	17.09
						12.07	27.42	20.51
						14.08	31.99	23.93
						16.09	36.56	27.35
						18.10	41.13	30.77
20.11	45.70	34.18						

6. The following compounds are considered as associates in thermodynamic modelling:

- metallic phase: Cr<sub>5</sub>Si<sub>3</sub>, FeSi, Fe, MnSi, Fe<sub>3</sub>Si, Cr, Mn<sub>3</sub>Si, Fe<sub>5</sub>Si<sub>3</sub>, Mn, CrSi, Mn<sub>5</sub>Si<sub>3</sub>, CrSi<sub>2</sub>, Cr<sub>3</sub>Si, Si, FeSi<sub>2</sub>, Al, CaSi, CaSi<sub>2</sub>, Mg, Al<sub>2</sub>Ca, Ca<sub>2</sub>Si, Al<sub>4</sub>Ca, Mg<sub>2</sub>Si, CaMg<sub>2</sub>

- slag phase: SiO<sub>2</sub>, Mn<sub>0.9554</sub>Ca<sub>0.0446</sub>SiO<sub>3</sub>, Mn<sub>2</sub>O<sub>3</sub>, Fe<sub>2</sub>O<sub>3</sub>, Mn<sub>2</sub>SiO<sub>4</sub>, MnO<sub>2</sub>, MnO, Cr<sub>2</sub>O<sub>3</sub>, MnSiO<sub>3</sub>, CaSiO<sub>3</sub>, Fe<sub>2</sub>MnO<sub>4</sub>, Mn<sub>3</sub>O<sub>4</sub>, CaO\*Al<sub>2</sub>O<sub>3</sub>\*2SiO<sub>2</sub>, Al<sub>2</sub>O<sub>3</sub>, MnO\*Al<sub>2</sub>O<sub>3</sub>, MnO\*Fe<sub>2</sub>O<sub>3</sub>, Fe<sub>3</sub>O<sub>4</sub>, Cr<sub>2</sub>FeO<sub>4</sub>, MgCr<sub>2</sub>O<sub>3</sub>, (CaFe)<sub>0.5</sub>SiO<sub>3</sub>, Fe<sub>0.945</sub>O, Fe<sub>0.947</sub>O, FeO, CaAl<sub>2</sub>SiO<sub>6</sub>, CaO\*Fe<sub>2</sub>O<sub>3</sub>, FeSiO<sub>3</sub>, FeAl<sub>2</sub>O<sub>4</sub>, MgSiO<sub>3</sub>, CaO\*Cr<sub>2</sub>O<sub>3</sub>, CaO\*Al<sub>2</sub>O<sub>3</sub>\*SiO<sub>2</sub>, FeO<sub>1.056</sub>, (CaMg)<sub>0.5</sub>SiO<sub>3</sub>, \*2CaO\*SiO<sub>2</sub>, MgO<sub>2</sub>, CaMgSi<sub>2</sub>O<sub>6</sub>, CaO\*Al<sub>2</sub>O<sub>3</sub>, CaO\*MgO\*2SiO<sub>2</sub>, MgO\*Al<sub>2</sub>O<sub>3</sub>, Ca<sub>3</sub>Si<sub>2</sub>O<sub>7</sub>, CaO\*MgO\*SiO<sub>2</sub>, MgFe<sub>2</sub>O<sub>4</sub>, \*3CaO\*2SiO<sub>2</sub>, \*2CaO\*Al<sub>2</sub>O<sub>3</sub>\*SiO<sub>2</sub>, MgO, CaFe(SiO<sub>3</sub>)<sub>2</sub>, CaO, \*3Al<sub>2</sub>O<sub>3</sub>\*2SiO<sub>2</sub>, \*2FeO\*SiO<sub>2</sub>, CaMgSiO<sub>4</sub>, FeO\*SiO<sub>2</sub>, CaO\*2Al<sub>2</sub>O<sub>3</sub>, Fe<sub>2</sub>MgO<sub>4</sub>, Ca<sub>3</sub>Fe<sub>2</sub>Si<sub>2</sub>O<sub>12</sub>, \*2CaO\*MgO\*2SiO<sub>2</sub>, CrO<sub>3</sub>, Mg<sub>2</sub>SiO<sub>4</sub>, \*2CaO\*Fe<sub>2</sub>O<sub>3</sub>, CrO<sub>2</sub>, Ca<sub>3</sub>SiO<sub>5</sub>, Al<sub>2</sub>O<sub>3</sub>\*2SiO<sub>2</sub>, \*3CaO\*Al<sub>2</sub>O<sub>3</sub>\*3SiO<sub>2</sub>, \*3CaO\*MgO\*2SiO<sub>2</sub>, CaO\*MgO, \*3CaO\*SiO<sub>2</sub>, Ca<sub>2</sub>MgSi<sub>2</sub>O<sub>7</sub>, Al<sub>4</sub>Mg<sub>2</sub>Si<sub>5</sub>O<sub>18</sub>, \*2CaO\*Al<sub>2</sub>O<sub>3</sub>, Mg<sub>2</sub>Al<sub>4</sub>Si<sub>5</sub>O<sub>18</sub>, Fe<sub>3</sub>Al<sub>2</sub>Si<sub>3</sub>O<sub>12</sub>, CaO\*6Al<sub>2</sub>O<sub>3</sub>, \*3CaO\*Al<sub>2</sub>O<sub>3</sub>, Fe<sub>2</sub>Al<sub>4</sub>Si<sub>5</sub>O<sub>18</sub>, CaCrO<sub>4</sub>, Mg<sub>3</sub>Al<sub>2</sub>Si<sub>3</sub>O<sub>12</sub>, MgCrO<sub>4</sub>, MgMn<sub>2</sub>O<sub>4</sub>, Cr<sub>2</sub>MgO<sub>4</sub>, MgCr<sub>2</sub>O<sub>4</sub>, CaFeSiO<sub>4</sub>, AlO, MgFe<sub>1.415</sub>Cr<sub>0.632</sub>O<sub>4.07</sub>, CaFe<sub>3</sub>O<sub>5</sub>, Cr<sub>3</sub>O<sub>12</sub>, Ca<sub>3</sub>Cr<sub>2</sub>(SiO<sub>4</sub>)<sub>3</sub>, Mg<sub>2</sub>Al<sub>4</sub>Si<sub>5</sub>O<sub>10</sub>, CaFe<sub>5</sub>O<sub>7</sub>, \*4CaO\*Al<sub>2</sub>O<sub>3</sub>\*Fe<sub>2</sub>O<sub>3</sub>, Mg<sub>7</sub>Al<sub>5</sub>O<sub>4</sub>\*Al<sub>9</sub>Si<sub>3</sub>O<sub>36</sub>, Cr<sub>8</sub>O<sub>21</sub>, \*12CaO\*7Al<sub>2</sub>O<sub>3</sub>, Ca(MnO<sub>4</sub>)<sub>2</sub>.

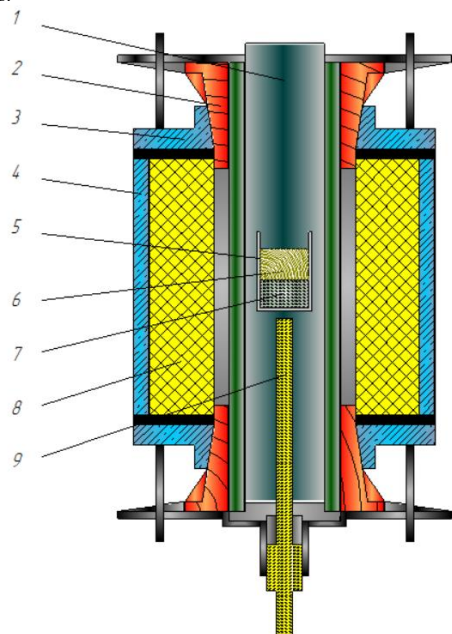
Based on theoretical data and the physicochemical properties of the charge materials discussed above, laboratory experiments were carried out in a Tamman furnace (**Fig. 1**) to establish the optimal temperature regime and to obtain an experimental sample of the chrome-manganese ligature.

The Tamman furnace is a high-temperature laboratory unit designed for simulating and studying metallurgical processes under controlled conditions. Its working chamber consists of a cylindrical graphite tube, which serves both as a heating element and a reaction zone due to its high electrical conductivity and thermal resistance. Temperature control is implemented via a precision thyristor voltage regulator [26–29], which is connected to the primary winding of a step-down transformer. This configuration enables the delivery of high current – up to several thousand amperes – to the furnace electrodes while maintaining a low voltage in the range of 0.5 to 15 V.

Such parameters ensure uniform and efficient resistive heating of the graphite tube, providing stable thermal conditions throughout the working zone. The furnace is capable of reaching operating temperatures in the range of 1800 to 2000 °C, with a maximum programmable heating rate of up to 25 °C per minute. Accurate temperature monitoring within the furnace is performed using a high-temperature tungsten-rhenium thermocouple (WRe-5/20), which is enclosed in a protective corundum (alumina) casing to shield it from the aggressive environment inside the furnace.

This advanced configuration makes the Tamman furnace particularly suitable for experimental melting, reduction, and alloy formation processes, especially in small-scale metallurgical research where precise control over thermal regimes is required. The ability to simulate high-temperature metallothermic reactions with reproducible parameters enables the assessment of phase formation, metal recovery rates, and slag behaviour under realistic operating conditions. Consequently, the furnace serves as a crucial tool for validating thermodynamic

models and optimising the technological parameters of innovative metallurgical processes.



1 – graphite tube; 2 – water-cooled copper plates; 3 and 4 – water-cooled housing; 5 – crucible; 6 – slag; 7 – metal; 8 – fireproof body; 9 – thermocouple

**Fig. 1** High-temperature resistance furnace (Tamman furnace)

To investigate the microstructural characteristics and elemental distribution in the obtained chrome-manganese ligature, a scanning electron microscope (SEM) “ZEPTOOLS – ZEM 20” (China) equipped with an integrated energy-dispersive X-ray spectroscopy (EDS) system was employed. This SEM system is capable of producing high-resolution images with magnifications of several thousand times, enabling detailed visualisation of surface morphology, phase boundaries, and the degree of structural homogeneity within the alloy.

The built-in EDS system, operating in tandem with the electron beam column, facilitates localised qualitative and semi-quantitative elemental analysis by detecting characteristic X-rays emitted from the specimen surface under electron beam excitation. This allows for precise identification of the elemental composition in micro-regions of interest.

The combination of SEM and EDS techniques enabled the identification of the spatial distribution of key alloying elements such as chromium, manganese, silicon, and iron within different regions of the metallic matrix. Both point analysis and elemental mapping were performed to evaluate the segregation tendencies of these elements and to detect the presence of intermetallic phases or residual oxide inclusions. The resulting micrographs and EDS spectra provided important insights into the structural integrity, phase morphology, and chemical uniformity of the synthesised chrome-manganese ligature.

## RESULTS AND DISCUSSION

The primary objective of the thermodynamic modelling conducted in this study is to determine the characteristic behaviour and redistribution patterns of chemical elements during the metallothermic reduction process, particularly focusing on their separation into the metallic and slag phases. The modelling aims to evaluate the stability of various oxide and intermetallic compounds formed under high-temperature conditions, as well as to quantify the extent to which valuable metals, such as chromium, manganese, and iron, are reduced and transferred into the metallic phase. Additionally, it provides insight into the composition and retention behaviour of elements such as silicon, aluminium, calcium, and magnesium within the slag system.

As a result of the thermodynamic calculations, it was established that during the smelting of chrome-manganese ligature by metallothermic methods, certain consistent trends in element redistribution and compound formation are observed,

depending on both temperature and the quantity of reducing agent introduced into the system (Fig. 2–4). These trends suggest that optimised thermal and compositional parameters play a crucial role in achieving effective separation between metal and slag, as well as in maximising the recovery of target alloying components.

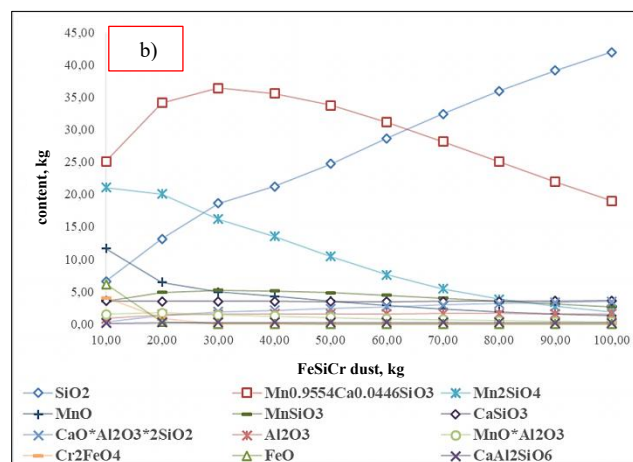
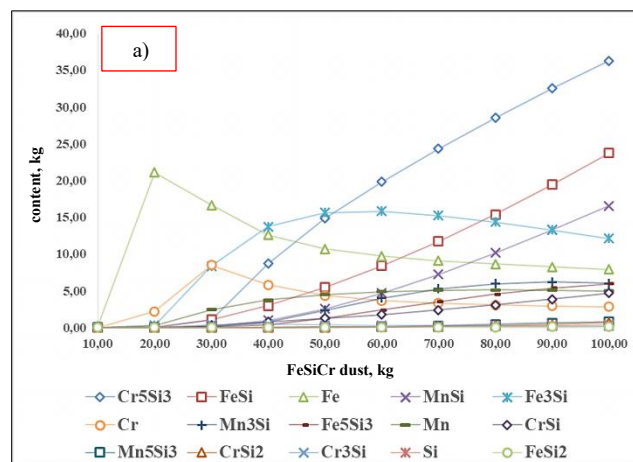


**Fig. 2** Dependence of the metallic (a) and slag (b) phases on the amount of FeSiCr dust at a temperature of 1400 °C

At 1400°C, with FeSiCr dust added in amounts ranging from 10 to 100 kg, the charge mixture exhibits notable transformations. Increasing the amount of the FeSiCr reducing agent from 10 to 100 kg leads to an intensive reduction of chromium, iron, and manganese oxides. This effect is especially evident for the oxide phase  $\text{Cr}_2\text{O}_3$ , whose quantity decreases from 11.6 kg at the lowest FeSiCr input to zero at just 40 kg. This indicates the high efficiency of silicon as a reductant, capable of displacing oxygen from stable Cr oxides even at moderate dosages.

Simultaneously, as the content of oxide phases declines, the amount of reduced metallic elements increases. The mass of metallic chromium reaches a peak of 8.46 kg at 30 kg of FeSiCr, after which it begins to decline – an effect attributed to further interaction of chromium with excess silicon, leading to the formation of silicides. Similar behaviour is observed for iron, which initially accumulates in its free form and later transitions into phases such as FeSi and  $\text{Fe}_2\text{Si}$ . Manganese also gradually reduces from oxides to its metallic form and subsequently forms silicides, such as MnSi.

At high FeSiCr dosages, the dominant transformation pathway becomes the formation of stable silicides. In particular, the  $\text{Cr}_5\text{Si}_3$  phase shows a sharp increase – from zero at 10 kg to 36.29 kg at 100 kg of FeSiCr. This suggests a redistribution of chromium from both its oxide and metallic forms into a silicide form under conditions of excess reductant. Thus, increasing the FeSiCr input not only

promotes the reduction of metals from oxides but also facilitates the formation of silicon-containing intermetallics, thereby stabilising the system at elevated temperatures. This behaviour is consistent with the thermodynamic favorability of silicide phases at high silicon activities, underscoring the need to balance reductant input to control the final alloy composition.

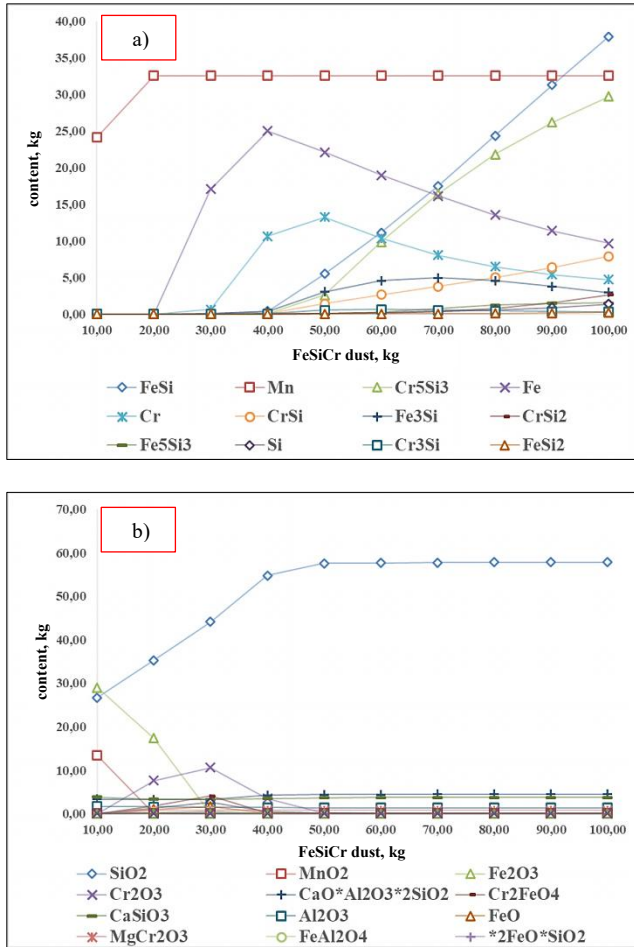


**Fig. 3** Dependence of the metallic (a) and slag (b) phases on the amount of FeSiCr dust at a temperature of 1600 °C

At a process temperature of 1600 °C, the behaviour of oxide reduction within the charge mixture demonstrates distinct and systematic changes when the amount of added FeSiCr dust is varied in the range of 10 to 100 kg. The introduction of FeSiCr significantly intensifies the reduction of chromium, iron, and manganese oxides, contributing to the progressive transformation of oxide compounds into their corresponding metallic forms. As the dosage of the reducing agent increases from 10 to 100 kg, a noticeable decline in the residual oxide content is observed, accompanied by a proportional growth in the metallic phase fraction, indicating a higher degree of reduction efficiency.

This reduction effect is particularly evident in the transformation behaviour of Cr<sub>2</sub>O<sub>3</sub>. At the minimum level of FeSiCr addition, the remaining mass of this oxide in the system is approximately 9.8 kg. However, with the increase in reductant dosage to approximately 30-40 kg, Cr<sub>2</sub>O<sub>3</sub> is fully reduced and eliminated from the oxide phase, demonstrating the high reductive capability of silicon under elevated thermal conditions. A similar trend of progressive oxide reduction is observed for iron and manganese oxides, specifically Fe<sub>2</sub>O<sub>3</sub> and MnO, which also undergo complete or near-complete conversion at higher reductant levels.

The depletion of oxides is accompanied by the accumulation of their respective metallic counterparts in the alloy phase. The mass of metallic chromium reaches a peak value of approximately 12.85 kg within the FeSiCr dosage range of 30-40 kg, confirming the effective reduction and separation. Additionally, the formation of

metallic iron and manganese intensifies with increasing amounts of the reducing agent, further supporting the overall reduction efficiency. These transformations reflect a sequential reduction mechanism in which oxides are reduced in stages to their metallic states, promoted by the stable thermal conditions at 1600 °C. This regime facilitates a more complete and directed transfer of valuable alloying components into the metallic phase.

At the same time, further increasing the amount of FeSiCr dust beyond 50-60 kg results in the redistribution of the already reduced metallic elements into more thermodynamically stable intermetallic compounds with silicon. Under such elevated reductant levels, the formation of silicide phases becomes increasingly prominent and structurally significant. Specifically, the Cr<sub>2</sub>Si<sub>3</sub> phase appears and exhibits a substantial increase, reaching up to 29.74 kg at the maximum FeSiCr addition. Comparable behaviour is noted for iron, as evidenced by the intensified formation of FeSi phases under conditions of elevated silicon activity, indicating a shift in equilibrium toward silicide stabilisation at high reductant excess.

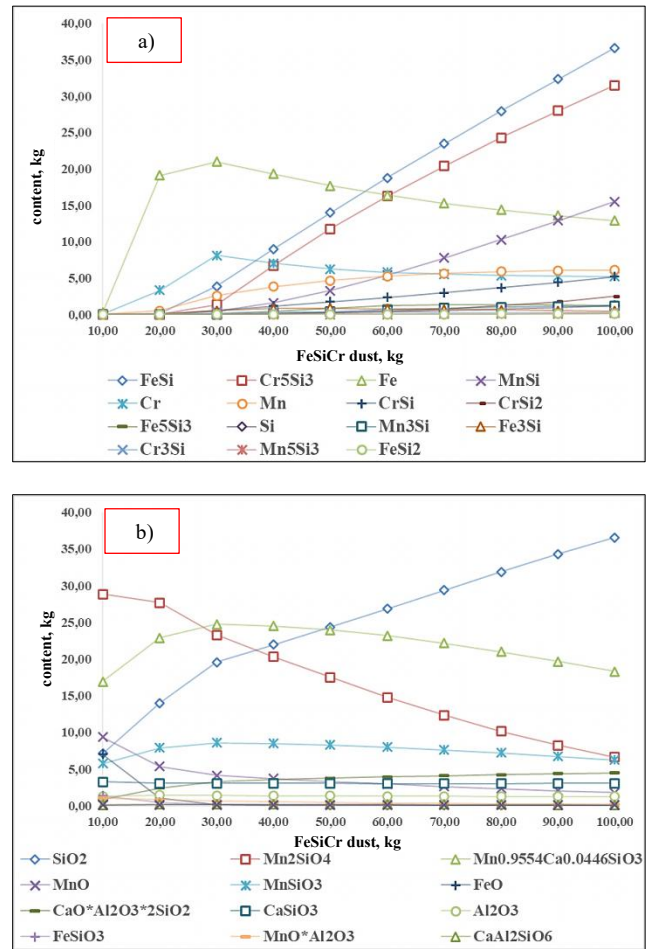


**Fig. 4** Dependence of the metallic (a) and slag (b) phases on the amount of FeSiCr dust at a temperature of 1800 °C

At a temperature of 1800 °C, with FeSiCr dust added in amounts ranging from 10 to 100 kg, the content of oxides such as Mn<sub>2</sub>SiO<sub>4</sub>, MnO, and Cr<sub>2</sub>O<sub>3</sub> decreases, indicating ongoing reduction processes. However, not all manganese is reduced to the metallic phase – a significant portion remains in the form of oxides. Simultaneously, an increase in SiO<sub>2</sub> content is observed, reaching 36.59 kg at 100 kg of FeSiCr, which indicates silica saturation in the slag. The complete disappearance of Cr<sub>2</sub>O<sub>3</sub> reflects the deep reduction of Cr under these conditions.

As the FeSiCr dosage increases, particularly beyond the 50 kg threshold, there is a marked intensification in the formation of intermetallic compounds involving iron, chromium, and silicon. The contents of silicide phases, such as Cr<sub>5</sub>Si<sub>3</sub>, CrSi, FeSi, and Fe<sub>5</sub>Si<sub>3</sub>, begin to rise significantly, demonstrating a clear shift in equilibrium

towards the stabilisation of silicide compounds rather than the accumulation of pure metallic phases. This transition is consistent with high silicon activity in the system and the thermodynamic preference for complex silicides under such reductive and thermal regimes.

Despite the favourable conditions for reduction at 1800 °C, the conversion of manganese into the metallic phase remains relatively limited. Even with the maximum input of 100 kg of FeSiCr, the amount of metallic Mn formed does not exceed 6.09 kg, while the formation of MnSi reaches only 15.53 kg. This limited recovery may be attributed not only to the incomplete reduction of manganese oxides but also to the potential evaporation of manganese at elevated temperatures, resulting in partial losses to the gas phase. Such behaviour highlights the volatility of manganese under extreme thermal conditions and underscores the challenge of achieving complete Mn recovery at 1800 °C.

According to the thermodynamic calculations, the compositions of the metal and slag phases were determined (Table 4), and the phase distribution trends of the main elements (Cr, Mn, Fe, etc.) were established as functions of temperature (1400–1800 °C) and the amount of reducing agent (dust FeSiCr) in the Fe-Cr-Mn-Si-Al-Ca-Mg-O system.

The calculations carried out enable the analysis of physicochemical processes occurring during the production of chrome-manganese ligature by metallothermic methods. It should be noted that the system under consideration is closed, meaning there is no interaction with the external environment.

Based on the results of the thermodynamic calculations, the metal recovery rates were determined as a function of both temperature and the amount of FeSiCr dust added to the charge mixture (Fig. 5–7). The modelling was carried out over a wide range of temperatures (1400–1800 °C) and FeSiCr input levels (10–100 kg), allowing for a comprehensive assessment of the reduction efficiency and phase formation under various conditions.

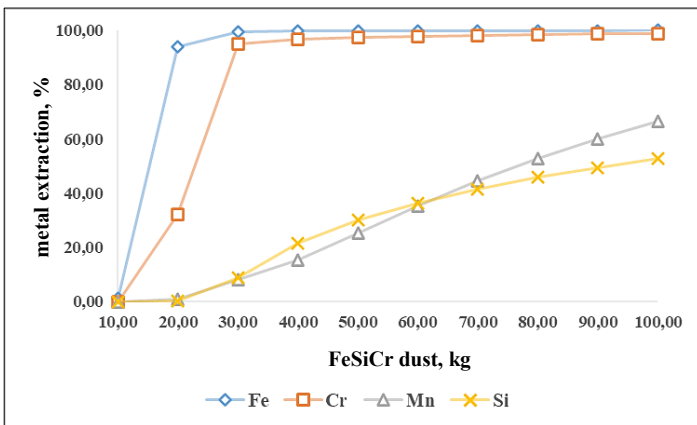


Fig. 5 Dependence of Fe, Cr, Mn, and Si recovery on the amount of FeSiCr dust at a temperature of 1400 °C

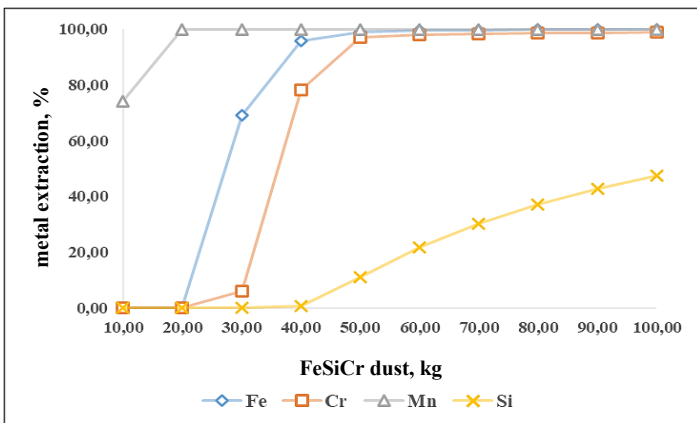


Fig. 6 Dependence of Fe, Cr, Mn, and Si recovery on the amount of FeSiCr dust at a temperature of 1600 °C

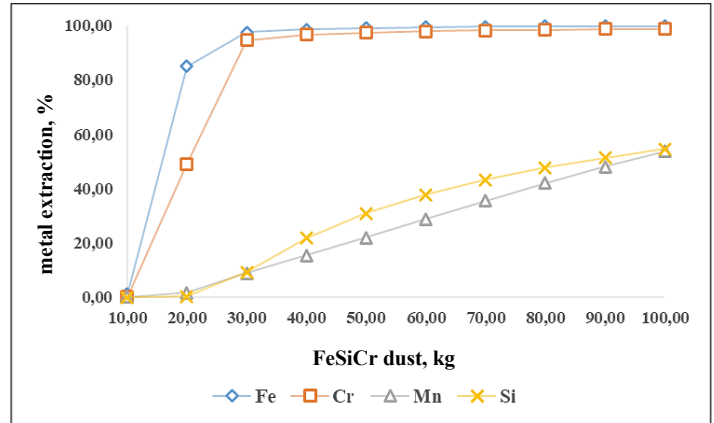


Fig. 7 Dependence of Fe, Cr, Mn, and Si recovery on the amount of FeSiCr dust at a temperature of 1800 °C

The results of the thermodynamic modelling indicate that the optimal set of process parameters corresponds to a temperature of 1600 °C and the addition of approximately 50 kg of FeSiCr dust. Under these conditions, the thermodynamic favorability of the system reaches its peak, and the kinetics of metallothermic reduction are sufficiently activated, thereby enabling the most complete transition of the target components from their oxide forms into the metallic phase. This combination of thermal and compositional parameters ensures a balanced relationship between energy sufficiency and reaction completeness, making 1600 °C a critical temperature point for efficient process implementation.

Under the identified optimal regime, the calculated recovery rates of the main metal components were as follows: Fe, 99.00%; Cr, 97.03%; Mn, 99.97%; and Si, 10.99%. These values demonstrate a near-total reduction of iron, chromium, and manganese oxides. The comparatively lower recovery of silicon is attributed to its partial retention within the slag phase and its involvement in the formation of thermodynamically stable silicide compounds.

Additionally, it should be noted that under these conditions, the calculated basicity index of the slag ( $\text{CaO}/\text{SiO}_2$ ) is approximately 1.8. This level of basicity is considered optimal for ensuring good slag fluidity, effective separation between metallic and slag phases, and stabilisation of silicate compounds. This further supports the favourable nature of phase interactions within the system and reinforces the high recovery efficiency of key alloying elements.

A comparative assessment of the metal recovery rates at boundary temperatures of 1400 °C and 1800 °C, relative to the optimal temperature of 1600 °C, clearly demonstrates the significant influence of thermal conditions on the efficiency of the metallothermic reduction process. At 1400 °C, the thermal energy is insufficient to drive the reduction reactions to completion, thereby limiting the conversion of chromium and manganese oxides into their metallic forms. This leads to suboptimal alloy composition and reduced recovery of the target elements. Conversely, at 1800 °C, although the reduction reactions proceed rapidly, the elevated temperature conditions can induce partial evaporation of manganese into the vapour phase, resulting in a measurable loss of this element from the metallic product. Such deviations from the thermal optimum disrupt the overall reduction balance and affect the homogeneity and yield of the final alloy.

Therefore, precise temperature control is crucial for maintaining the desired thermodynamic conditions and maximising process efficiency. The thermodynamically derived data provide a robust scientific basis for further laboratory-scale validation and technological fine-tuning. These results enable the minimisation of experimental uncertainty and support the development of stable and efficient smelting regimes for producing high-quality chrome-manganese ligatures with maximised elemental recovery.

Table 4 Chemical composition of metal and slag

T=1400 °C									
FeSiCr dust, kg	Metal composition, kg				Slag composition, kg				
	Fe	Cr	Mn	Si	SiO <sub>2</sub>	CaO	FeO	Al <sub>2</sub> O <sub>3</sub>	MnO
10	0.25	0.00	0.00	0.00	28.89	52.00	22.49	3.12	41.86
20	21.32	2.21	0.27	0.04	39.56	71.20	1.38	3.11	41.45
30	24.53	9.75	2.58	2.04	45.29	81.53	0.08	3.11	38.45
40	26.60	13.22	5.00	5.95	46.71	84.09	0.04	3.11	35.33
50	28.63	16.65	8.17	9.69	48.47	87.25	0.02	3.11	31.25
60	30.66	20.07	11.48	13.41	50.30	90.54	0.01	3.11	26.99
70	32.68	23.49	14.52	17.20	51.98	93.56	0.01	3.11	23.07
80	34.69	26.92	17.22	21.09	53.47	96.24	0.01	3.11	19.59
90	36.71	30.34	19.57	25.06	54.77	98.58	0.01	3.10	16.55
100	38.73	33.76	21.60	29.11	55.89	100.61	0.01	3.10	13.92
T=1600 °C									
FeSiCr dust, kg	Metal composition, kg				Slag composition, kg				
	Fe	Cr	Mn	Si	SiO <sub>2</sub>	CaO	FeO	Cr <sub>2</sub> O <sub>3</sub>	Al <sub>2</sub> O <sub>3</sub>
10	0.00	0.00	24.11	0.00	30.22	54.39	0.00	6.58	3.12
20	0.00	0.00	32.55	0.00	39.19	70.55	2.64	9.40	3.13
30	17.07	0.62	32.55	0.00	48.67	87.60	4.99	13.41	3.13
40	25.56	10.69	32.55	0.21	58.65	105.57	0.57	3.69	3.13
50	28.39	16.58	32.55	3.56	61.48	110.66	0.11	0.08	3.13
60	30.51	20.06	32.55	8.07	61.63	110.93	0.06	0.01	3.13
70	32.58	23.49	32.55	12.61	61.70	111.05	0.04	0.00	3.13
80	34.64	26.91	32.55	17.16	61.74	111.13	0.02	0.00	3.13
90	36.68	30.34	32.55	21.71	61.77	111.19	0.02	0.00	3.13
100	38.71	33.76	32.55	26.26	61.80	111.23	0.01	0.00	3.13
T=1800 °C									
FeSiCr dust, kg	Metal composition, kg				Slag composition, kg				
	Fe	Cr	Mn	Si	SiO <sub>2</sub>	CaO	MnO	FeO	Al <sub>2</sub> O <sub>3</sub>
10	0.25	0.00	0.00	0.00	0.00	0.00	0.00	0.00	0.00
20	19.24	3.35	0.52	0.06	29.47	53.05	41.93	25.15	3.14
30	24.02	9.70	2.86	2.12	39.44	70.99	41.22	3.91	3.14
40	26.29	13.21	5.00	6.03	45.02	81.04	38.18	0.68	3.14
50	28.41	16.64	7.16	9.99	46.45	83.61	35.42	0.38	3.14
60	30.49	20.07	9.37	13.96	47.72	85.89	32.64	0.26	3.14
70	32.54	23.49	11.56	17.94	48.98	88.16	29.78	0.19	3.14
80	34.58	26.91	13.66	21.95	50.21	90.38	26.96	0.15	3.14
90	36.62	30.34	15.63	26.00	51.38	92.49	24.26	0.12	3.14
100	38.65	33.76	17.46	30.08	52.48	94.47	21.72	0.10	3.14

## Smelting and Results

Based on the results of thermodynamic calculations, a charge mixture with a total mass of 100 g was prepared, consisting of 43.00 g of ferro-manganese ore, 22.00 g of FeSiCr dust, and 35.00 g of lime (CaO). CaO was added as a flux to bind acidic components during slag formation and to regulate its basicity.

Before smelting, the mixture was thoroughly homogenised manually in a porcelain mortar until a uniform mass was obtained. This ensured even distribution of the components within the crucible volume, thereby promoting uniform progress of reduction and phase transformation reactions during heating. The homogenised mixture was then loaded into an alumina crucible.

The Tamman furnace was heated to 1600 °C, a temperature selected based on thermodynamic modelling results, which indicated that the maximum recovery of Cr, Mn, and Fe occurs at this temperature with minimal formation of silicide phases. The charge was held at this temperature for 20 minutes, providing sufficient time for reduction reactions to occur and for the metallic and slag phases to form. After the smelting process was completed, the crucible was removed and cooled to room temperature. Fig. 11 shows the appearance of the solidified smelting products - chrome-manganese ligature and the corresponding slag.

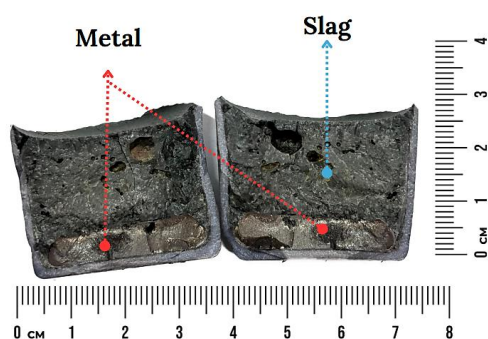


Fig. 8 Products of high-temperature smelting of the chrome-manganese ligature

As shown in Fig. 8, the metal and slag are separated. It should be noted that no significant gas evolution was observed during the smelting process. The resulting slag exhibited a solid, stony structure. The ratio of the formed slag (72.40 g) to metal (28.50 g) was 2.54.

## Microstructural and Phase Analysis

A microstructural examination of the chrome-manganese ligature sample was conducted, along with an EDS analysis of the microstructural components. Fig. 9 shows the images obtained in backscattered electron detection mode, as well as elemental distribution maps of the main elements present in the ligature.

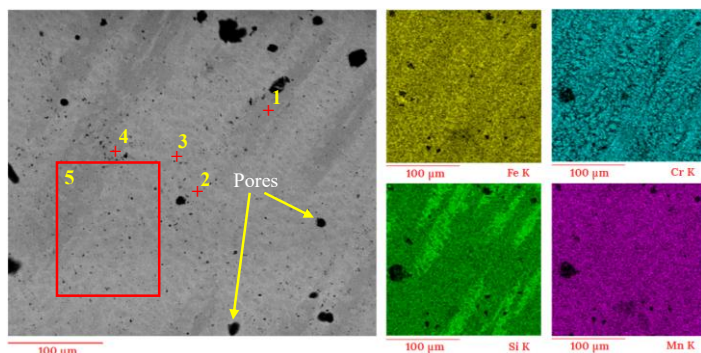


Fig. 9 SEM image of the chrome-manganese ligature and elemental distribution map

The images obtained using SEM enabled the investigation of the microstructure of the chrome-manganese ligature. For the analysis, five different regions of the sample were selected, in which spectral analysis was performed (Table 3).

Table 3 Content of major elements in different spectra (based on EDS analysis)

Area, №	Content, wt.%				
	Fe	Cr	Mn	Si	Al
1	38.02	14.48	23.64	14.48	-
2	52.89	6.29	25.67	15.15	-
3	34.56	28.40	25.03	12.01	-
4	45.56	3.98	22.86	12.07	0.30
5	40.95	19.08	25.89	14.08	-

The results showed that the main elements – Fe, Cr, Mn, and Si – are unevenly distributed across the surface of the ligature. The concentrations of Fe and Cr vary significantly in different areas, indicating a heterogeneous composition. At the same time, the contents of Mn and Si remain relatively stable. This elemental distribution suggests the presence of local zones with differing chemical compositions, which may be due to phase separation or insufficient mixing of the components during the ligature formation process. Additionally, pores of various sizes are visible on the surface, indicating a certain degree of porosity in the structure and possible peculiarities of the technological process.

The slag phase consists mainly of calcium aluminosilicate ( $\text{CaO} \cdot \text{Al}_2\text{O}_3 \cdot 2\text{SiO}_2$ ), along with  $\text{SiO}_2$  and CaO oxides, and contains a minimal amount of  $\text{Al}_2\text{O}_3$  (1.26%).

## CONCLUSION

Based on the conducted thermodynamic modelling, it was established that the most optimal conditions for the smelting of chrome-manganese ligature are achieved at a temperature of 1600 °C with the addition of 50 kg of FeSiCr dust per 100 kg of manganese ore. Under these conditions, the maximum reduction of Cr and Mn is achieved. The resulting composition of the metal phase is as follows (in kg): Fe – 28.39, Cr – 16.58, Mn – 32.55, Si – 3.56. These parameters can be recommended for further laboratory research.

A crucible smelting experiment was carried out at 1600 °C with a holding time of 20 minutes. As a result, a solid, rock-like slag was formed. Laboratory studies confirmed the feasibility of using FeSiCr dust as a reductant in the production of chrome-manganese ligature, as well as the potential to obtain a new complex alloy. Further research under industrial conditions, along with the establishment of large-scale production of this alloy, will enable the utilisation of low-grade Mn ores and more accessible reductants, thereby increasing the economic efficiency of ferroalloy production.

Additionally, SEM analyses were performed to determine the microstructure of the obtained ligature. The results revealed a heterogeneous distribution of the main elements (Fe, Cr, Mn, Si). The resulting slag had the structure of calcium aluminosilicate ( $\text{CaO} \cdot \text{Al}_2\text{O}_3 \cdot 2\text{SiO}_2$ ).

**Acknowledgements:** This research is funded by the Science Committee of the Ministry of Education and Science of the Republic of Kazakhstan (Grant No. AP23488918)

## REFERENCES

- Ye. Makhambetov, N. Timirbayeva, S. Baisanov, A. Baisanov, E. Shabanov: *Metalurgija*, 60(1–2), 2021, 117–120.
- M.I. Druinsky, V.I. Zhuchkov: *Production of complex ferroalloys from mineral raw materials of Kazakhstan*, Alma-Ata: Nauka, 1988, 208 p. (in Russian).
- V.N. Shashkin, N.M. Loginov, T.A. Bagautdinov, A.F. Fursenko, B.K. Utemisov: *Gornyi Zhurnal*, 11, 2021, 32–34.
- I.R. Manashev: Utilisation of dispersed ferroalloys by the SHS method. In *Physicochemical Fundamentals of Metallurgical Processes Named After Academician A.M. Samarin*, Vykxa, Russia, 2022, p. 364.
- W. Wei, P.B. Samuelsson, P.G. Jönsson, R. Gyllenram, B. Glaser: *JOM*, 75, 2023, 1206–1220. <https://doi.org/10.1007/s11837-023-05880-4>
- T.Z. Zhukebayeva, K.A. Akhmediyeva, E.M. Zholdangarov: *StudNet*, 3, 2020, 615–620.
- R. Dlamini, H. von Blottnitz: *Minerals*, 13, 2023, 44. <https://doi.org/10.3390/min13010044>

8. Ye. Shabanov, Ye. Kuatbay, Ye. Makhambetov, R. Toleukadyr: Engineering Journal of Satbayev University, 144(6), 2022, 11-17. <https://doi.org/10.51301/ejsu.2022.i6.02>
9. L. Yang, J. Liu, X. Hua, H. Wang: Resources, Conservation and Recycling, 209, 2024, 107816. <https://doi.org/10.1016/j.resconrec.2024.107816>
10. O. Sariyev, B. Kelamanov, Ye. Zhumagaliyev, S. Kim, A. Abdirashit, M. Almagambetov: Metalurgija, 59(4), 2020, 533-536.
11. O. Sariyev, et al.: Materials, 18(4), 2025, 903. <https://doi.org/10.3390/ma18040903>
12. Y. Makhambetov, A. Zhakan, S. Gabdullin, A. Akhmetov, A. Burumbayev, A. Zhunusov: Acta Metallurgica Slovaca, 31(2), 2025, 113-118. <https://doi.org/10.36547/ams.31.2.2137>
13. S.K. Nath: Construction and Building Materials, 181, 2018, 487-494. <https://doi.org/10.1016/j.conbuildmat.2018.06.070>
14. G. Zhang, Y. Sun, Y. Xu: Renewable and Sustainable Energy Reviews, 82, 2018, 477-487. <https://doi.org/10.1016/j.rser.2017.09.072>
15. A. Abdirashit, et al.: Metals, 15(4), 2025, 428. <https://doi.org/10.3390/met15040428>
16. Y. Yu, et al.: Metallurgical and Materials Transactions B: Process Metallurgy and Materials Processing Science, 54, 2023, 2370-2382. <https://doi.org/10.1007/s11663-023-02838-w>
17. H.G. Castellanos, et al.: Journal of Water Process Engineering, 59, 2024, 104987. <https://doi.org/10.1016/j.jwpe.2024.104987>
18. O. Sariyev, et al.: Materials, 18(11), 2025, 2608. <https://doi.org/10.3390/ma18112608>
19. C. Ren, et al.: Materials, 16, 2023, 2385. <https://doi.org/10.3390/ma16062385>
20. Y. Gao, et al.: Northwestern Geology, 56, 2023, 142-155. <https://doi.org/10.12401/j.nwg.2022006>
21. A. Zhakan, A. Zhunusov, A. Akhmetov, S. Kabyllkanov, O. Yucel: Nauka i Tekhnika Kazakhstana, 4, 2024, 245-262. <https://doi.org/10.48081/MJRO9482>
22. Ye. Makhambetov, S. Gabdullin, A. Zhakan, Zh. Saulebek, A. Akhmetov, Z. Zulhan, S. Mukanov: Materials Research Express, 11(5), 2024, 056523. <https://doi.org/10.1088/2053-1591/ad4f58>
23. B. Akhmetzhanov, K.B. Tazhibekova, A.A. Shametova: Bulletin of Karaganda University, Series Economics, 4(92), 2018, 63-69, (in Russian).
24. Ye.N. Makhambetov, S.T. Gabdullin, Z. Zulhan, A.M. Zhakan, A.A. Myrzagaliyev: Nauka i Tekhnika Kazakhstana, 3, 2023, 211-221. <https://doi.org/10.48081/ODXD9913>
25. G. Adilov, A.D. Povolotsky, V.E. Roshchin: Chernaya Metallurgiya, 65(8), 2022, 581-589. <https://doi.org/10.17073/0368-0797-2022-8-581-589>
26. B. Kelamanov, et al.: Metalurgija, 61(3-4), 2022, 771-773.
27. A. Roine: Outokumpu HSC Chemistry for Windows: *Chemical reaction and equilibrium software with extensive thermochemical database*. Outokumpu Research OY, 2002.
28. J. Zhang, et al.: Metals, 14(12), 2024, 1378. <https://doi.org/10.3390/met14121378>
29. A. Akhmetov, et al.: Processes, 13, 2025, 1745. <https://doi.org/10.3390/pr13061745>